Electronic Supplementary Material (ESI) for ChemComm.

Tandem catalysis by ultrathin metal-organic nanosheets formed through post-synthetic functionalisation of a layered framework

Supplementary Information (SI)

Joshua Nicks, Zhang Jiawen and Jonathan A. Foster*

University of Sheffield, Department of Chemistry, Sheffield, S3 7HF, UK

Contents

S1. General Details

S1.1. Materials

Commercial solvents, reagents and spectroscopic grade deuterated solvents were used as purchased without further purification. Solvothermal synthesis of Cu(ABDC)(DMF) was carried out using borosilicate vials with Teflon-lined caps in a Carbolite Gero PF 60 Oven. Post-synthetic functionalisations were carried out in dry glassware with a nitrogen overpressure.

S1.2. Analytical Procedures

Elemental analyses were performed by the microanalytical service at the Department of Chemistry, University of Sheffield using a Vario MICRO Cube in an atmosphere of pure O_2. Elemental contents are determined to a tolerance of ± 0.5 % for organometallics.

FT-IR spectra were recorded using a Perkin Elmer Spectrum 100 FT-IR spectrophotometer, equipped with a SenseIR diamond ATR module. Samples were analysed without further preparation, and spectra were obtained in reflectance mode between 4000 – 600 cm^{-1}, using 12 scans with a spectral resolution of 1 cm^{-1}.

NMR spectra were recorded at 300 K using a Bruker Avance III HD 400 spectrometer equipped with a standard geometry 5mm BBFO probe with a single z-gradient at 400 MHz (^1H). Supramolecular frameworks were digested prior to submission, using DCl (23 µL) and DMSO-d_6 (1 mL). Mass spectra were recorded directly from NMR solutions using an Agilent 6530 QTOF LC-MS in negative ionization mode.

UV-vis absorption spectra were obtained on a Varian Cary 50 Bio spectrophotometer using standard 1 cm width quartz cells and Perkin Elmer Spectrum One software. Spectral data was formatted using Excel.

Powder X-ray diffraction data were collected using a Bruker-AXS D8 diffractometer using Cu K_α (λ=1.5418 Å) radiation and a LynxEye position sensitive detector in Bragg Brentano parafocussing geometry using a packed glass capillary or a flat silicon plate.

Thermogravimetric analyses were performed using a Perkin-Elmer Pyris 1 instrument. Approximately 4 mg of sample was weighed into a ceramic pan, held under nitrogen flow of 20 cm^3 min^{-1} at 25 °C for 10 minutes to purge the sample and allow for equilibration, then

ramped to varying end temperatures (see individual traces for details) at 1 °C min^{-1}. The samples were then held at the final temperature for 10 minutes to allow sample burn off.

DLS data were collected using a Malvern Zetasizer Nano Series particle size analyser, using a He-Ne laser at 633 nm, operating in backscatter mode (173 °). Samples were equilibrated at 298 K for 60 s prior to analysis. Zeta potential data were collected using the same instrument in zeta potential mode, using disposable polycarbonate capillary electrophoresis cells and according to the Smoluchowski method. Contact angle measurements were obtained using a Ramé-Hart Goniometer and coated mica surfaces.

Atomic force microscopy images were recorded using a Bruker Multimode 5 Atomic Force Microscope, operating in soft-tapping mode in air under standard ambient temperature and pressure, fitted with Bruker OTESPA-R3 silicon cantilevers operated with a drive amplitude of ~18.70 mV and resonance frequency of ~236 kHz. Samples were prepared by drop-casting 10 µL drops of suspension onto the centre of freshly cleaved mica sheets heated to 100 °C on a hot plate. These sheets were stuck to stainless steel, magnetic Agar scanning probe microscopy specimen discs. Images were processed using Gwyddion software.

S2. Synthetic Procedures

S2.1 Synthesis of Cu(ABDC)(DMF)

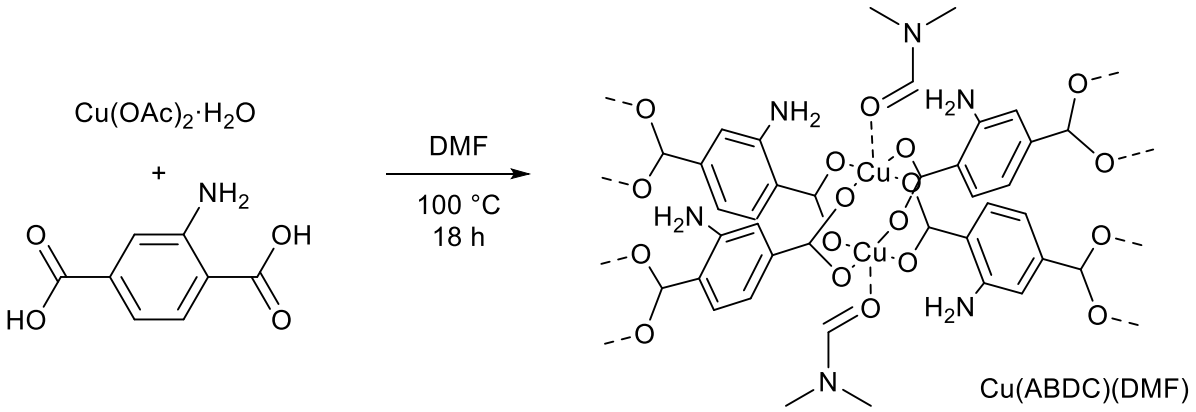

Copper acetate monohydrate (250.1 mg, 1.25 mmol) and 2-aminoterepthallic acid (229.1 mg, 1.26 mmol) were each dissolved in DMF (50 mL) and added in equal aliquots to 10 reaction vials. Reaction vials were then heated in a reaction oven to 100 °C at a rate of 1.0 °C min^{-1}, maintained for 18 hours, then cooled to 25 °C at a rate of 0.1 °C min^{-1}. Reaction mixtures were combined and centrifuged (4500 rpm, 30 mins), after which the supernatant was pipetted off and the wet solid washed with DMF (2 x 15 mL) and diethyl ether (2 x 10 mL). The sample was dried in air giving copper 2-aminoterephthalate (Cu(ABDC)(DMF) (382.3 mg, 1.20 mmol, 96 %) as a green powder. Elemental analysis: calculated mass for $CuC_{11}H_{12}O_5N_2$ %: C 41.82; H 3.83; N 8.87; Found mass %: C 41.46; H 4.02 N 8.79; MS (ESI-NEG): 180.0 $[M]^-$, 136.0 $[M - CO_2]^-$, 92.1 $[M - 2(CO_2)]^-$; phase purity was confirmed by PXRD (capillary) comparison to MOF-46.

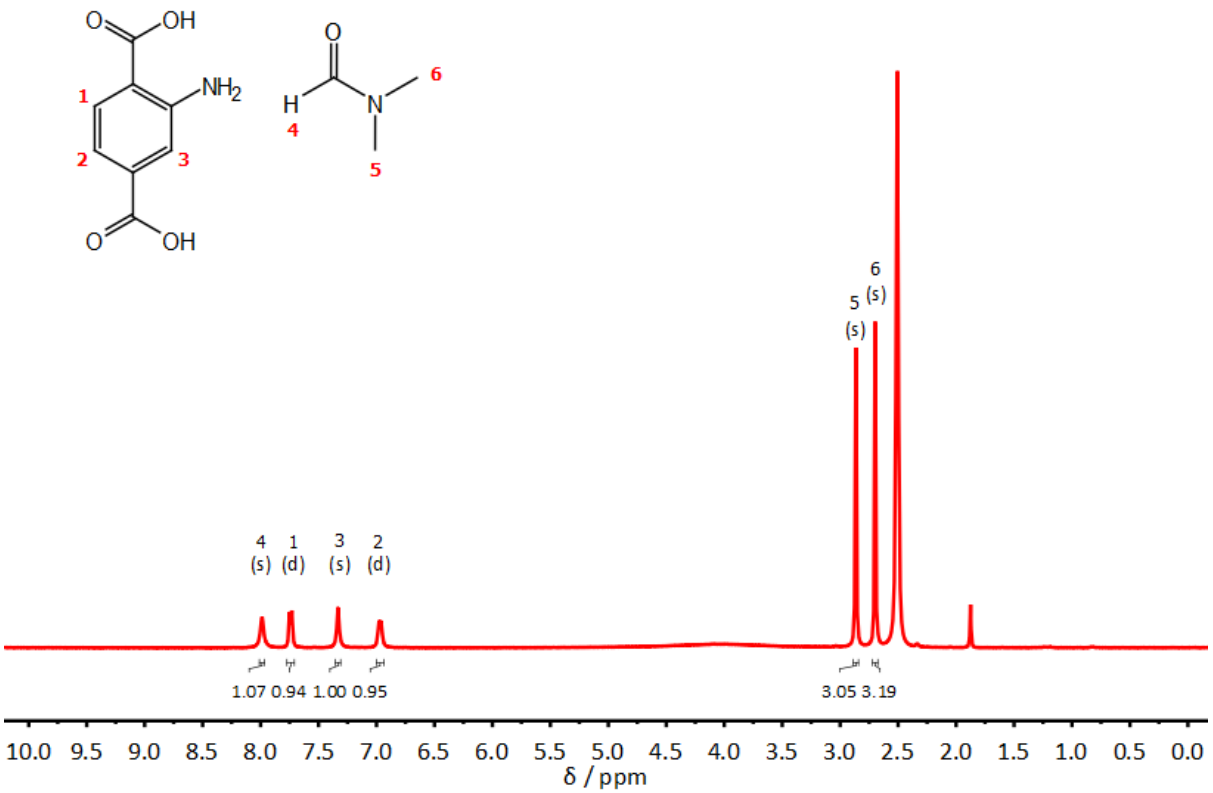

Figure S1. ^{1}H NMR spectrum of Cu(ABDC)(DMF) digested with DCl/DMSO-d_6, with peaks assigned according to the inset molecular structures. The unassigned peak at 1.90 ppm corresponds to residual acetate.

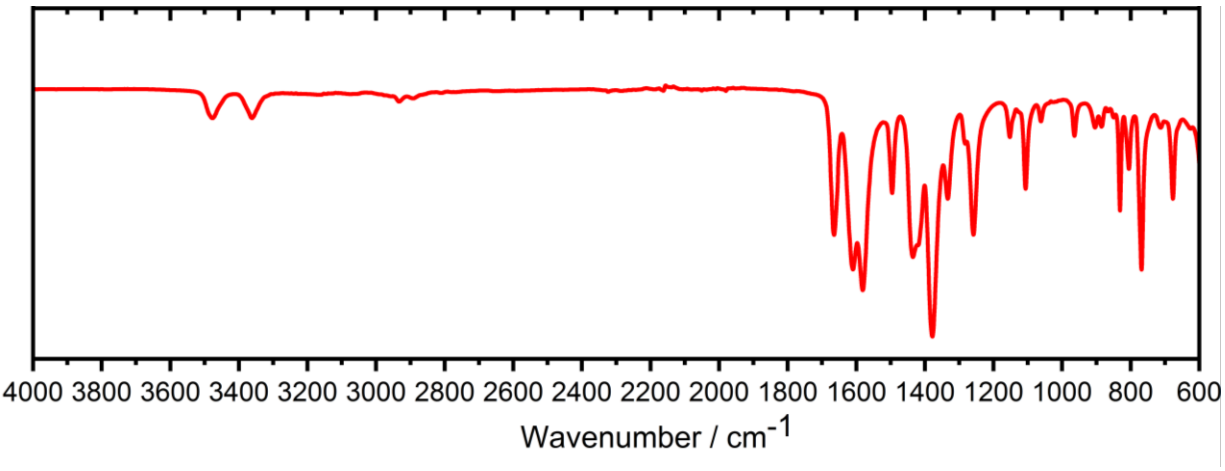

Figure S2. ATR-IR spectrum of Cu(ABDC)(DMF).

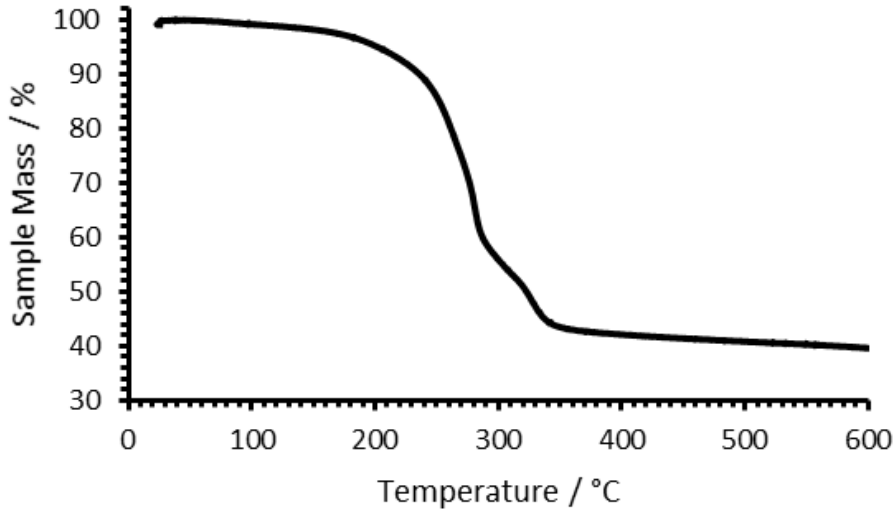

Figure S3. TGA plot for Cu(ABDC)(DMF).

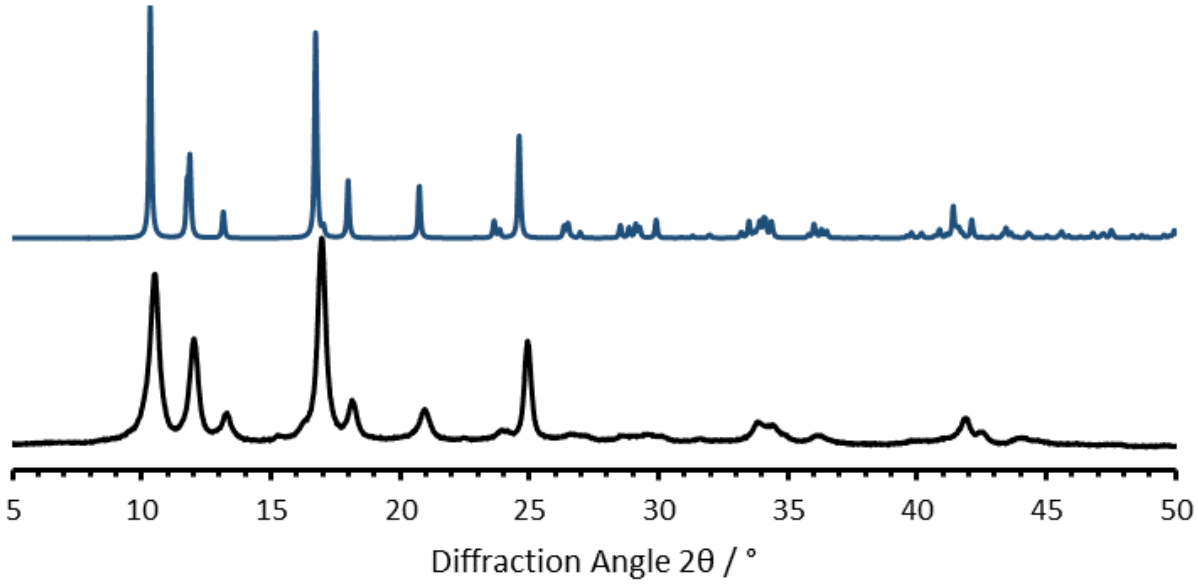

Figure S4. PXRD pattern obtained from Cu(ABDC)(DMF) (recorded in capillary mode) compared to a pattern calculated from the analogous Zn(ABDC)(DMF), MOF-46.[1]

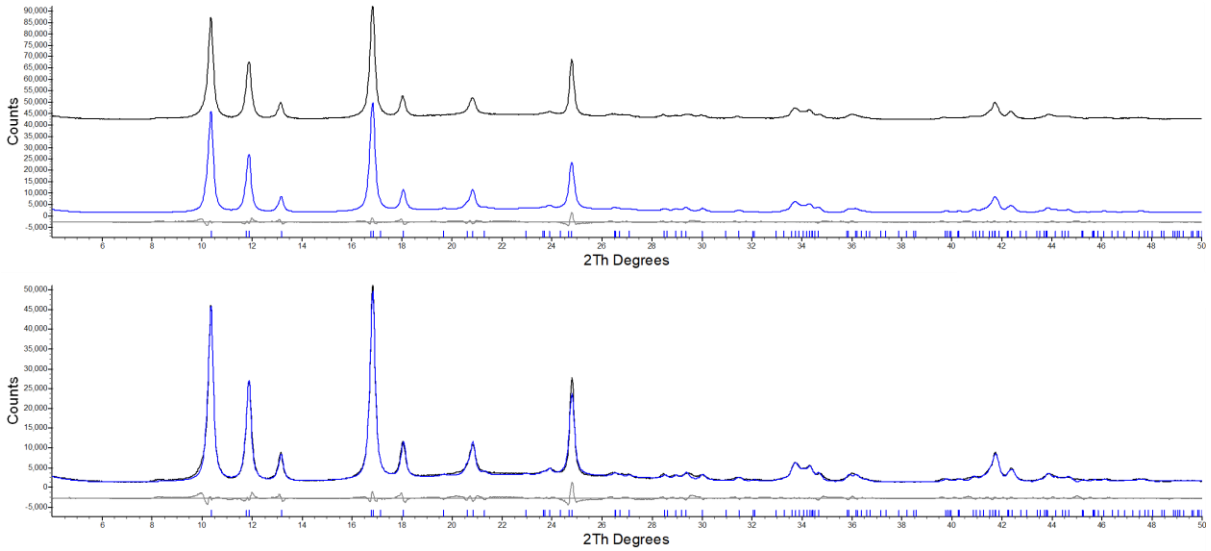

Figure S5. Pawley fit of the X-ray diffraction pattern of Cu(ABDC)(DMF) to MOF-46, stacked (top) and superimposed (bottom). Blue, black and grey lines represent calculated, experimental and difference profiles respectively. Tick marks indicate positions of allowed Bragg reflections in the space group C2/m.

Table S1. Crystallographic data of the Cu(ABDC)(DMF) MOF determined by Pawley refinement of PXRD data. Reference data for MOF-46 is also included.

	MOF-46 [1]	**Cu(ABDC)(DMF)**
Space Group	C2/m	C2/m
a / Å	11.2043(9)	11.1420(6)
b / Å	15.0516(12)	15.0305(4)
c / Å	8.0275(7)	8.0132(8)
β / °	111.7060(10)	111.8223(7)
R_{wp}		7.264
R_{exp}		1.635

S2.2. Post-synthetic functionalisation of Cu(ABDC)(DMF) with 1,3-propanesultone – Cu(ABDC-PS)(DMF)

Cu(ABDC)(DMF) (99.9 mg, 0.32 mmol) was suspended in chloroform (10 mL) and treated with 1,3-propanesultone (391.0 mg, 3.20 mmol, 280 µL) under a N_2 atmosphere. The suspension

was then heated under reflux at 55 °C for one week. The resulting suspension was centrifuged (4500 rpm, 1 hour) and the supernatant was pipetted off. The wet solid was then washed with chloroform (10 mL x3) and centrifuged (4500 rpm, 30 mins), after which the supernatant was removed. The sample was then washed with DMF (10 mL x 3) and diethyl ether (10 mL x 2) in the same way and left to dry in air, giving Cu(ABDC-PS)(DMF) as a light green powder (109.8 mg, 17 % conversion). Elemental analysis: Calculated mass for [0.17 Cu(ABDC-PS) + 0.83 Cu(ABDC) + 1.1 DMF + 0.08 $C_3H_6SO_3$] calc. from ^{1}H NMR] %: C 40.66; H 4.07; N 8.12; S 2.83; Found mass %: C 37.85; H 4.12 N 7.35; S 3.99; 1H NMR (DCl/DMSO-d_6): 7.97 (s, 1H, **DMF**), 7.84 (d, 1H, ArC*H* (**ABDC-PS**), *J* 8.0 Hz), 7.77 (d, 1H, ArC*H* (**ABDC**), *J* 8.0 Hz), 7.37 (s, 1H, ArC*H* (**ABDC**)), 7.23 (s, 1H, ArC*H* (**ABDC-PS**)), 7.06 (d, 1H, ArC*H* (**ABDC-PS**), *J* 8.0 Hz), 7.02 (d, 1H, ArC*H* (**ABDC**), *J* 8.0 Hz), 3.28 (m, 2H, CH_2 (**ABDC-PS)**), 2.87 (s, 3H, **DMF**), 2.71 (s, 3H, **DMF)**, 1.87 (m, 2H, CH_2 (**ABDC-PS))** ppm; MS (NEG-ESI): 424.0 $[M + SO_3H]^-$, 302.0 $[M]^-$, 180.0 $[ABDC]^-$.

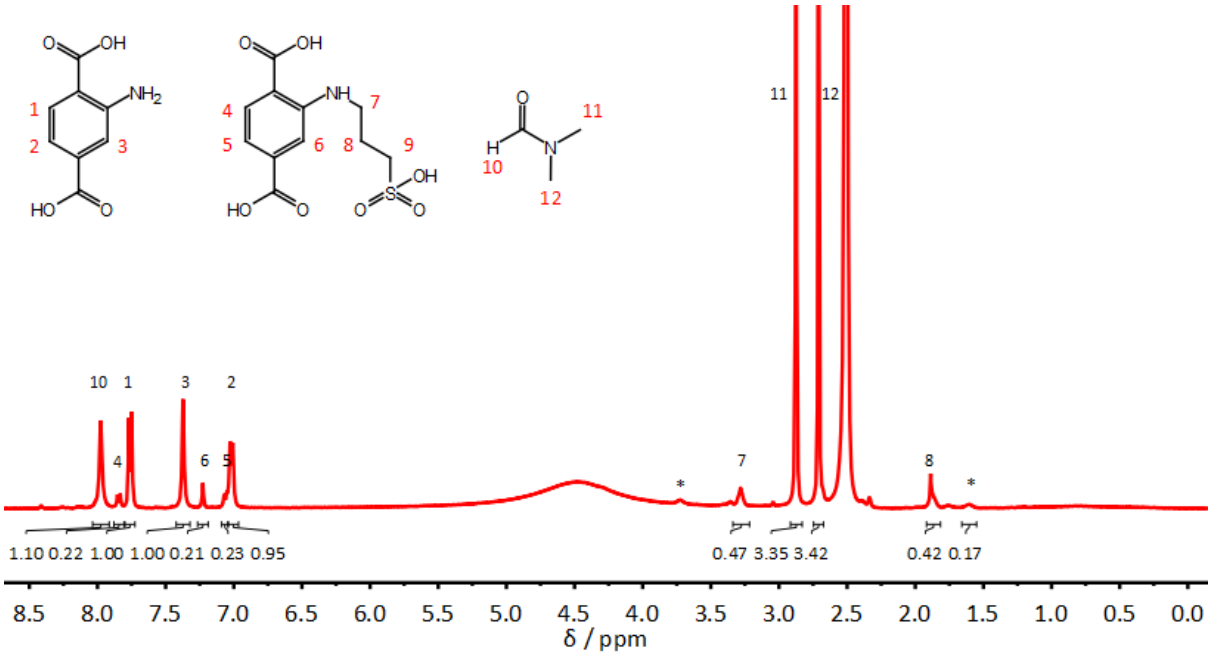

Figure S6. ^{1}H NMR spectrum of Cu(ABDC-PS)(DMF) digested with DCl/DMSO-d_6, showing a 17:83 ratio of the functionalised ligand to ABDC. A peak for the proton environment labelled 9 could not be assigned as it is masked by the residual solvent peak. Peaks marked with an * indicate small amounts of 3-hydroxypropane-1-sulfonic acid, which forms in the NMR solvent system due to hydrolysis of terminal acids which have reacted with 1,3-propanesultone.

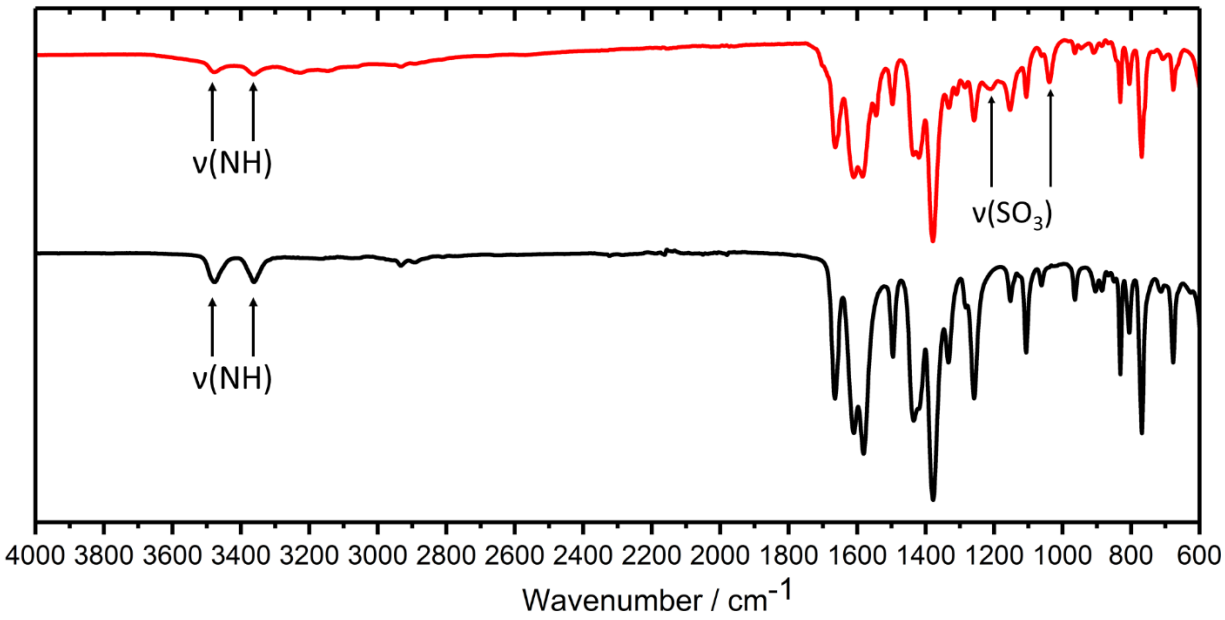

Figure S7. Infra-red spectrum of Cu(ABDC-PS)(DMF) (red) compared to Cu(ABDC)(DMF) (black), including two new bands associated with sulfonic acid stretches, as well as weak stretches in the 3200-3000 cm^{-1} region associated with the introduced C-H bonds.[2–4]

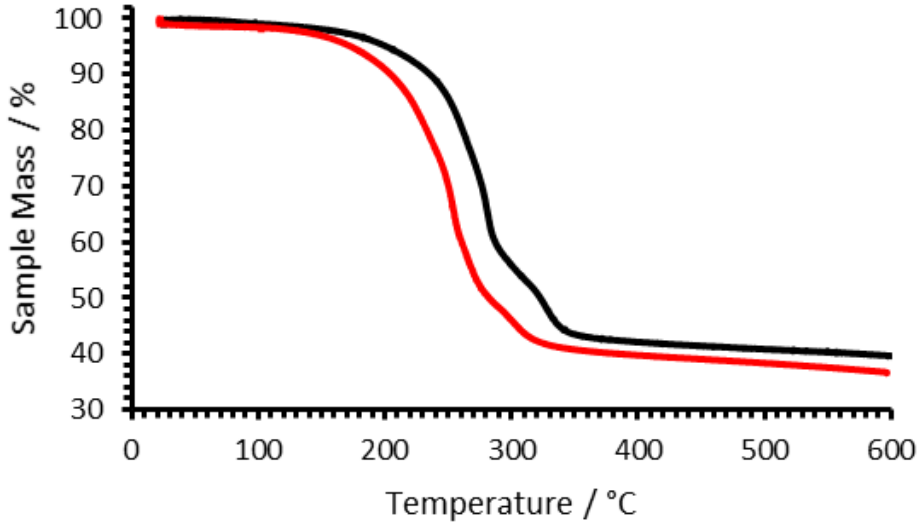

Figure S8. TGA plot of Cu(ABDC-PS)(DMF) (red) compared to Cu(ABDC)(DMF) (black).

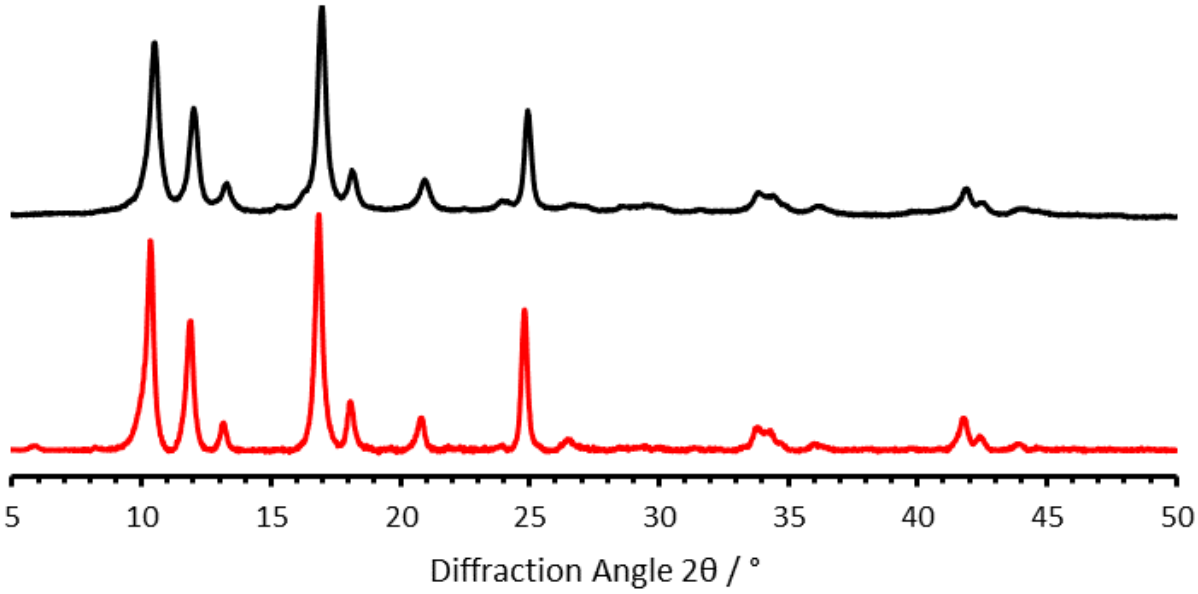

Figure S9. PXRD pattern obtained from Cu(ABDC-PS)(DMF) (red) (recorded in capillary mode) compared to the pattern obtained from Cu(ABDC)(DMF) (black), which indicates that phase and phase purity have been maintained.

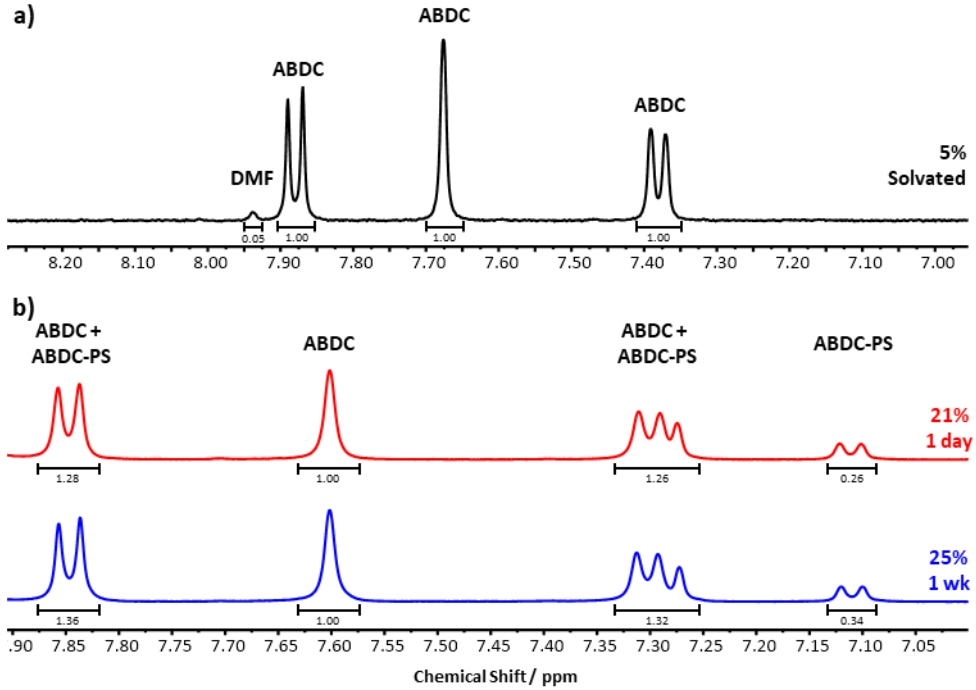

Figure S10. 1H NMR spectra of: a) desolvated Cu(ABDC) MOF which indicates only 5% solvation after soaking in acetonitrile for 3 days, b) products obtained from PSF of desolvated Cu(ABDC) for 1 day (red) and 1 week (blue), indicating 21 and 25 % functionalisation respectively.

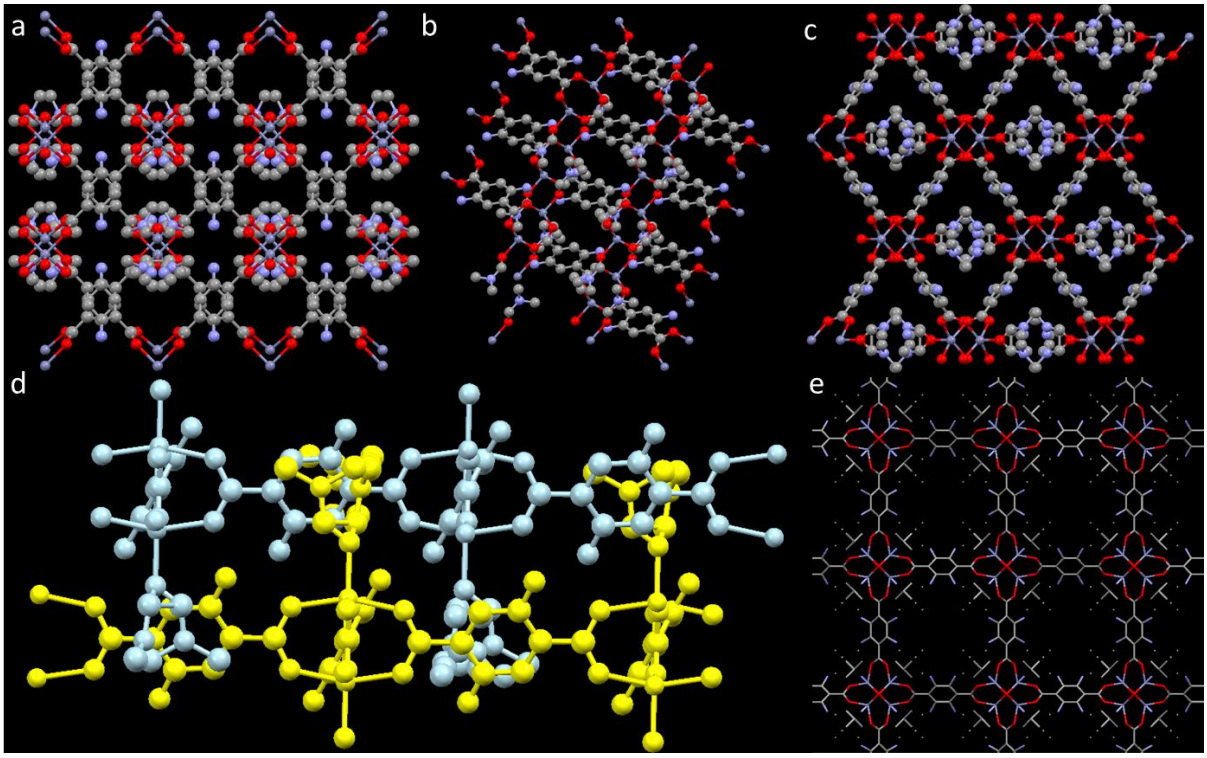

Figure S11. Ball and stick representations of single crystal structure of Zn(ABDC)(DMF) viewed along the hkl planes a) 100, b) 010 c) 001,[1] and d) through the layers, with adjacent layers highlighted in blue and yellow.[1] e) IRMOF-3, a Zn-O-C cluster based MOF with aminoterepthalate linkers that extend in 3D showing larger accessible pores in these systems, viewed from the hkl plane 100.[5]

S3. Exfoliation Studies

S3.1. Ultrasonic Exfoliation Method

Liquid-assisted ultrasonic exfoliations were carried out by suspension of 5 mg of MOF in 6 mL of acetonitrile inside a 10 mL reaction vial. The sample was mixed in a vortex mixer for 30 seconds to disperse the sediment. The samples were sonicated using a Fisherbrand Elmasonic P 30H ultrasonic bath (2.75 L, 380/350 W, UNSPSC 42281712) filled with water. Samples were sonicated for 12 hours at a frequency of 80 kHz with 100% power and the temperature was thermostatically maintained at 16-20°C using a steel cooling coil. Sonication was applied using a sweep mode and samples were rotated through the water using an overhead stirrer to minimise variation due to ultrasound "hot-spots" in accordance with a previously reported set-up.[6] Suspensions of nanosheets were obtained by centrifugation at 1500 rpm for 1 hour, followed by removal of the suspension from the isolated bulk powder.

S3.2. Tyndall Scattering

After sonication and exfoliation, samples of both Cu(ABDC)(DMF) and Cu(ABDC-PS)(DMF) exhibited Tyndall scattering effects, as shown in figure S11.

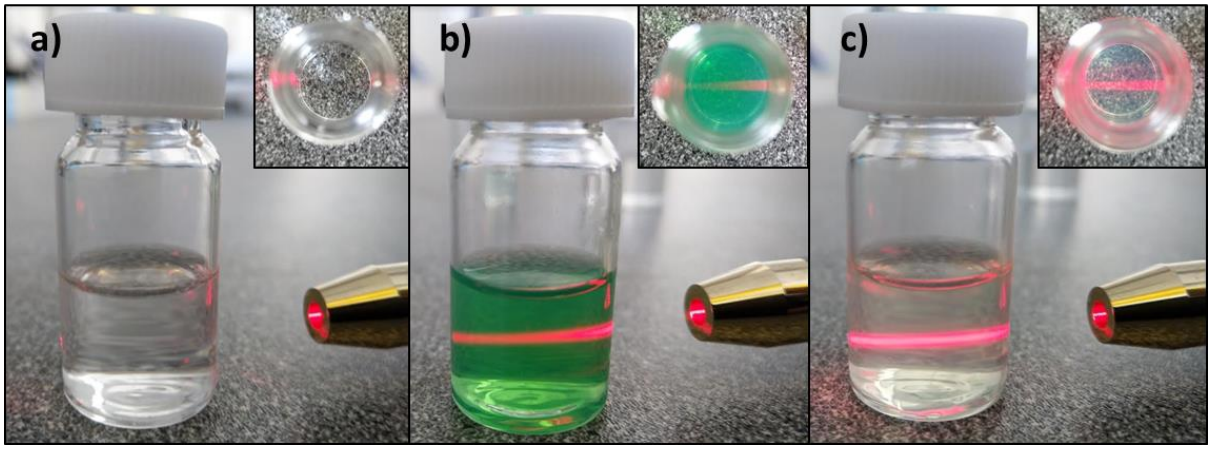

Figure S12. From left to right: profile and inset top-down images showing Tyndall scattering effects of a) acetonitrile and suspensions of b) Cu(ABDC)(DMF) and c) Cu(ABDC-PS)(DMF) following exfoliation in acetonitrile.

S3.3. Post-Exfoliation PXRD

In order to confirm that the supramolecular structure had been maintained post-exfoliation, powder X-ray diffraction patterns were obtained of nanosheet samples after exfoliation. Both patterns were recorded in flat plate mode due to the low mass obtained.

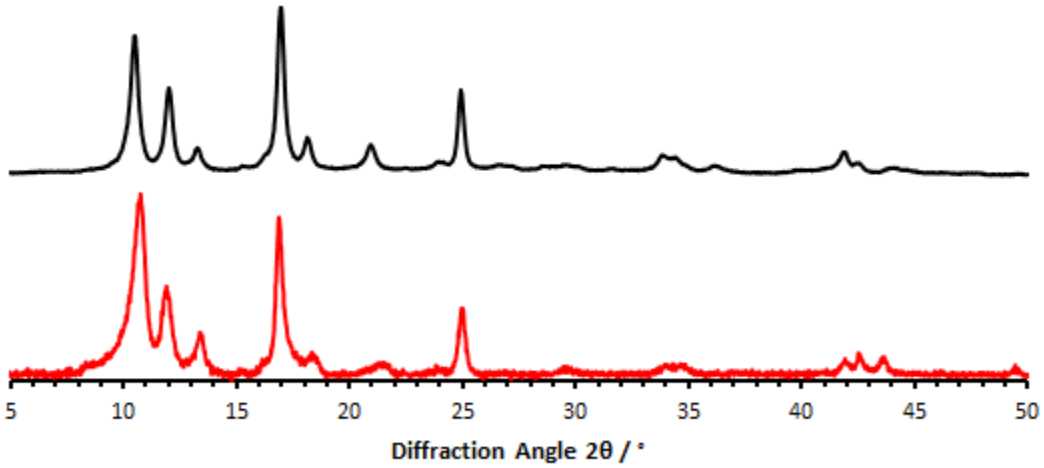

Figure S13. PXRD of Cu(ABDC)(DMF) before (black), after exfoliation (red) in acetonitrile. Sample obtained by centrifugation of nanosheet suspension at 4500 rpm for 3 hours.

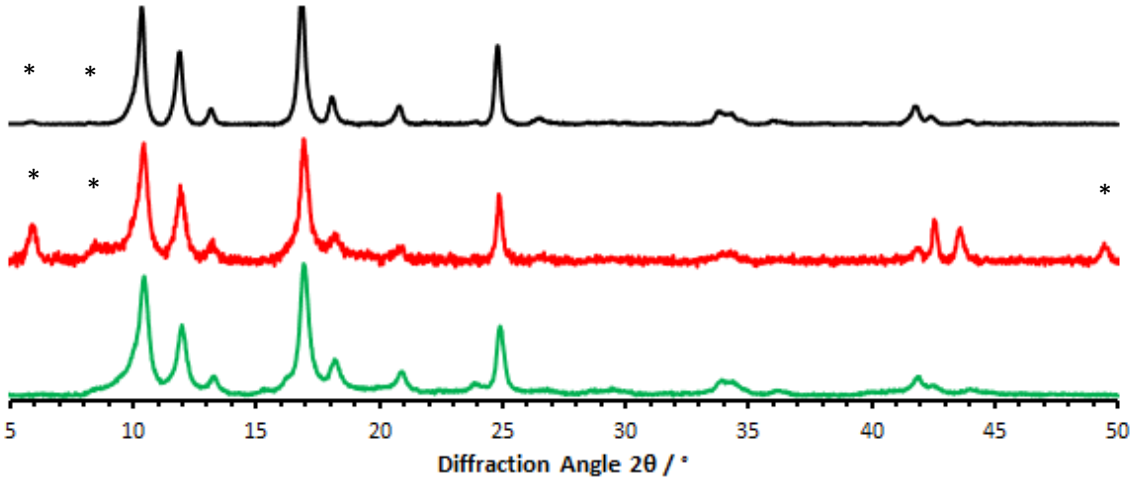

Figure S14. PXRD of Cu(ABDC-PS)(DMF) before (black), after exfoliation (red) in acetonitrile. Sample obtained by centrifugation of nanosheet suspension at 4500 rpm for 3 hours. * Peaks belonging to a minor phase were observed at 6, 8 and 50°, most prominently in the red exfoliated pattern. Trace amounts of this phase are also observed in the unexfoliated and unfunctionalised material. The MONs were redispersed in DMF (6 mL) using a vortex mixer for 30 seconds, and soaked for 18 h, centrifuged at 4500 rpm for 30 min, washed with diethyl ether. The resulting XRPD pattern (green) no-longer shows this minor phase which is attributed to a desolvated phase caused by loss of DMF from the axial sites of the MON as seen in related materials.[6,7] This is consistent with NMR data shown in Figure S23 which shows lower than expected DMF concentrations in the MONs which are restored in the material which has been soaked in DMF.

S3.4. Dynamic Light Scattering

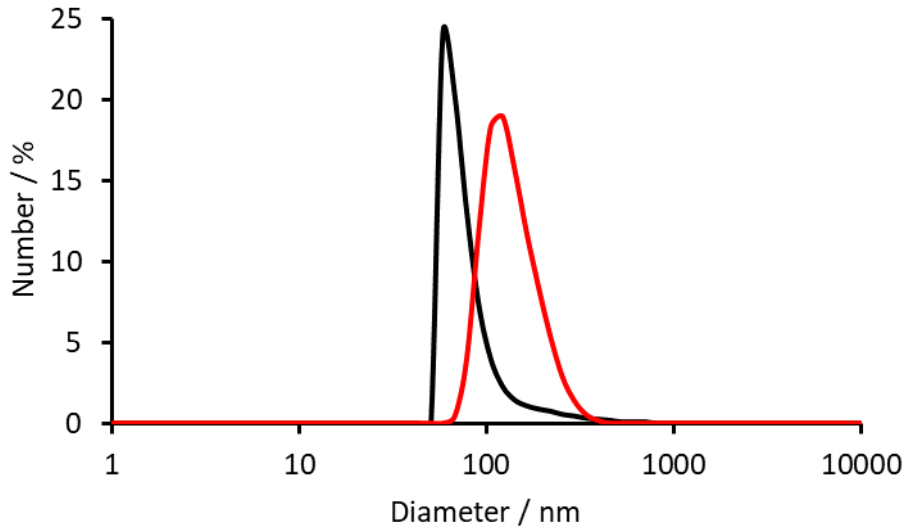

Figure S15. DLS number plot for MON suspensions of Cu(ABDC)(DMF) (black) and Cu(ABDC-PS)(DMF) (red). Suspensions were each diluted by a factor of 10 before analysis.

Table S2. Zeta potential data obtained using the Smoluchowski method.

Sample Name	T (°C)	ZP (mV)	Standard Deviation Frequency (Hz)	Zeta Deviation (mV)	Mobility (µmcm/Vs)	Mobility Deviation (µmcm/Vs)	Derived Count Rate (kcps)
Cu(ABDC) 1	20	-23.0	4.10	17.8	-0.4129	0.3184	1159.8
Cu(ABDC) 2	20	-23.3	3.52	15.3	-0.4175	0.2735	778.5
Cu(ABDC) 3	20	-22.3	3.95	17.1	-0.3991	0.3065	1241.2
Cu(ABDC) 4	20	-22.5	3.88	16.8	-0.4042	0.3018	2015.3
Cu(ABDC) 5	20	-24.0	4.46	19.3	-0.4302	0.3461	1374.4
	Avg	-23.0					
Cu(ABDC-PS) 1	20	-40.9	4.72	20.4	-0.7324	0.3666	1212.9
Cu(ABDC-PS) 2	20	-40.1	4.54	19.7	-0.7192	0.3526	1351.6
Cu(ABDC-PS) 3	20	-40.3	3.22	14.0	-0.723	0.2502	1125.3
Cu(ABDC-PS) 4	20	-40.2	3.85	16.7	-0.7206	0.2994	1041.6
Cu(ABDC-PS) 5	20	-36.7	3.47	15.0	-0.6575	0.2692	1778.1
	Avg	-39.6					

S3.5. UV-Vis Concentration Studies

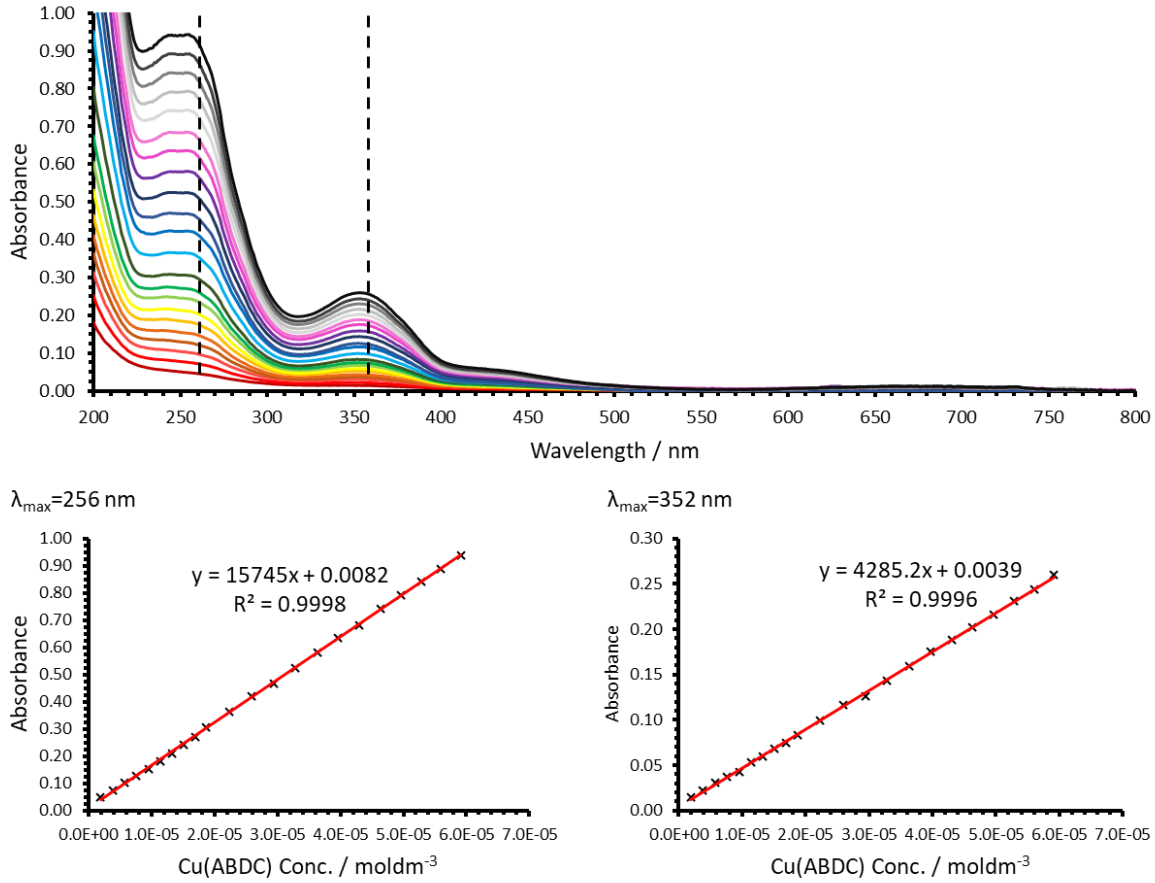

Figure S16. UV-Vis stack plot and extinction coefficient calculation graphs for Cu(ABDC)(DMF) in acetonitrile.

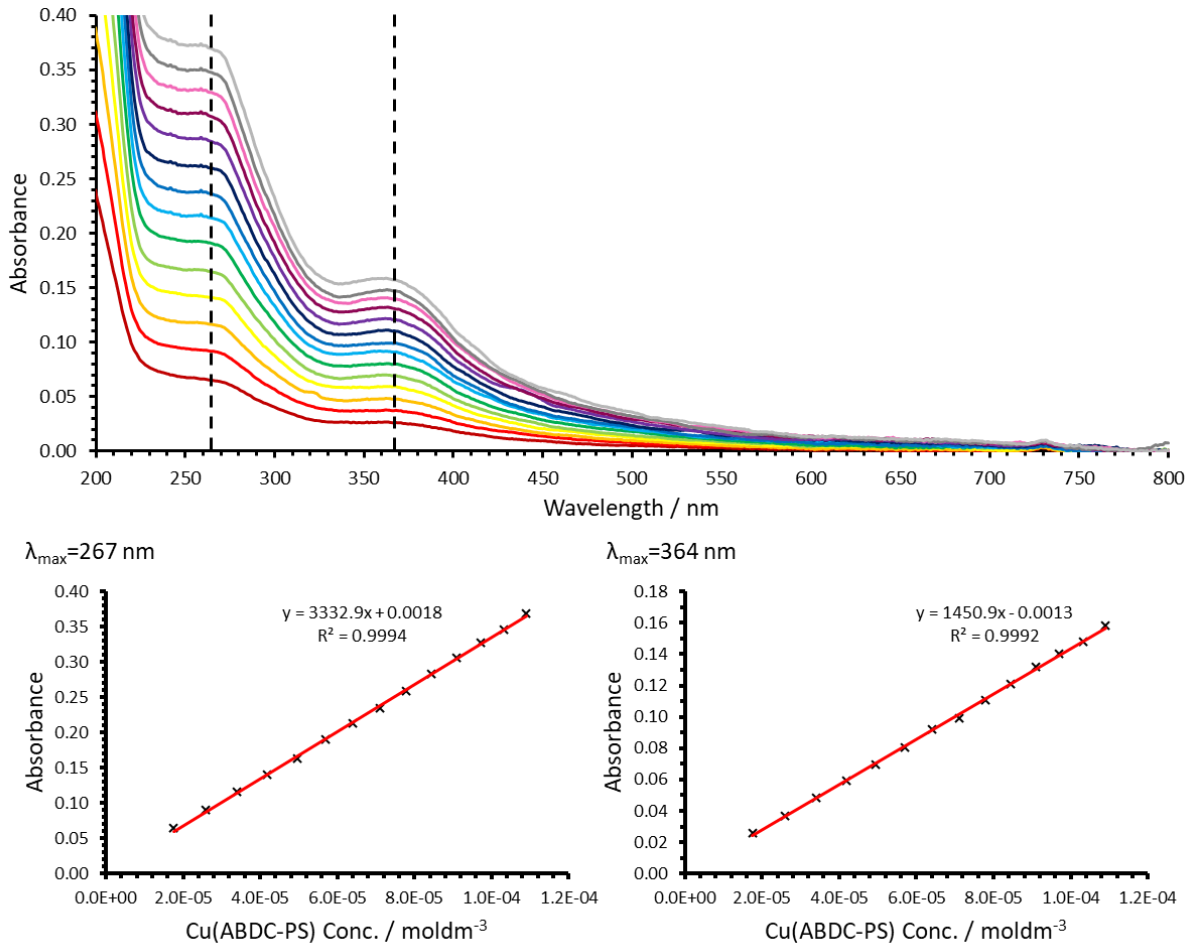

Figure S17. UV-Vis stack plot and extinction coefficient calculation graphs for Cu(ABDC-PS)(DMF) in acetonitrile.

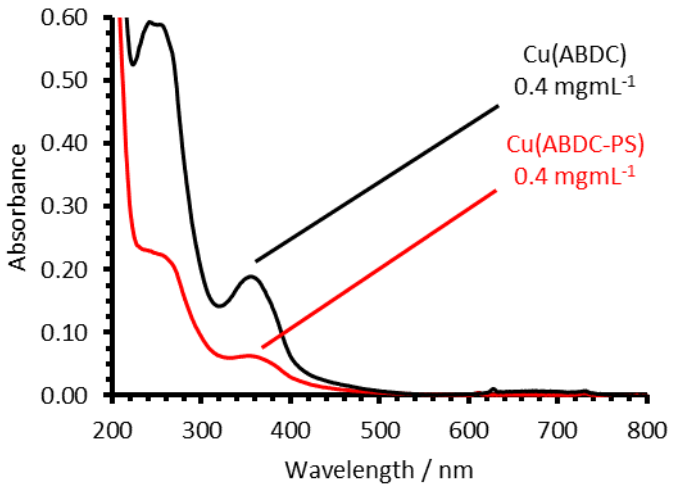

Figure S18. UV-Vis spectra of MON suspensions of Cu(ABDC)(DMF) (black) and Cu(ABDC-PS)(DMF) red, with concentrations highlighted as according the above extinction coefficients.

S3.6. Atomic Force Microscopy

S3.6.1. Exfoliation of Cu(ABDC)(DMF)

Shown in figure S19, nanosheets obtained from ultrasonic exfoliation of Cu(ABDC)(DMF) had a thickness distribution of 25 nm ±19 and a lateral size distribution of 175 nm ±48.

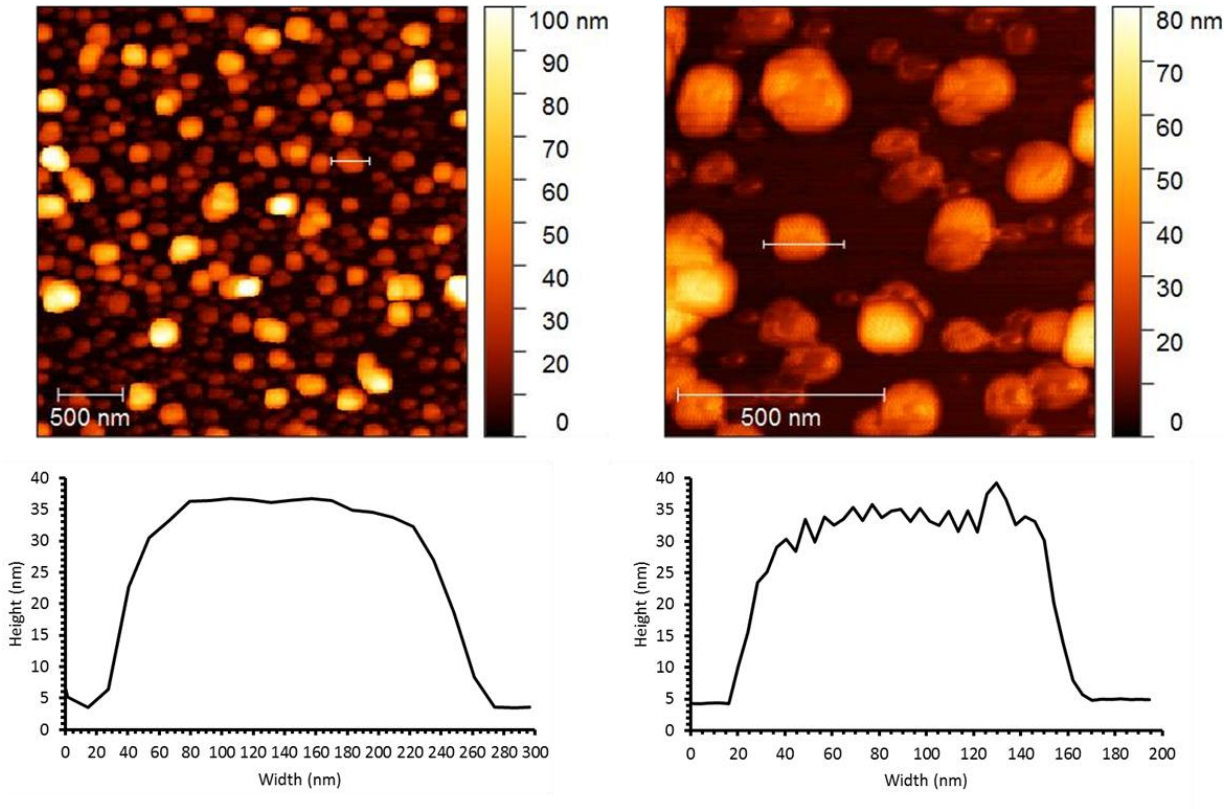

Figure S19. Atomic force microscopy images of exfoliated nanosheets of Cu(ABDC)(DMF) and associated height profiles.

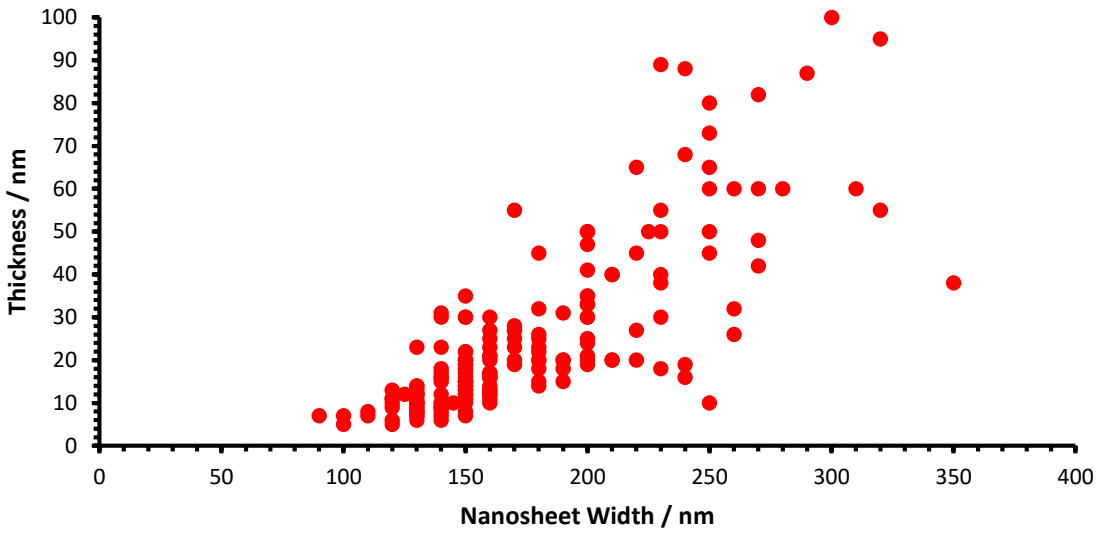

Figure S20. Size distribution scatter graph of Cu(ABDC)(DMF) nanosheets calculated from the above images.

3.6.2. Exfoliation of Cu(ABDC-PS)(DMF)

Nanosheets obtained from ultrasonic exfoliation of Cu(ABDC-PS)(DMF) were all consistently ~1.4 nm in thickness, with some exceptions that appeared to exhibit restacking or adsorption of particulates to the surfaces and some small amounts of unexfoliated material. Lateral sizes ranged typically from 100-400 nm, and nanosheets had irregular morphologies due to fracturing.

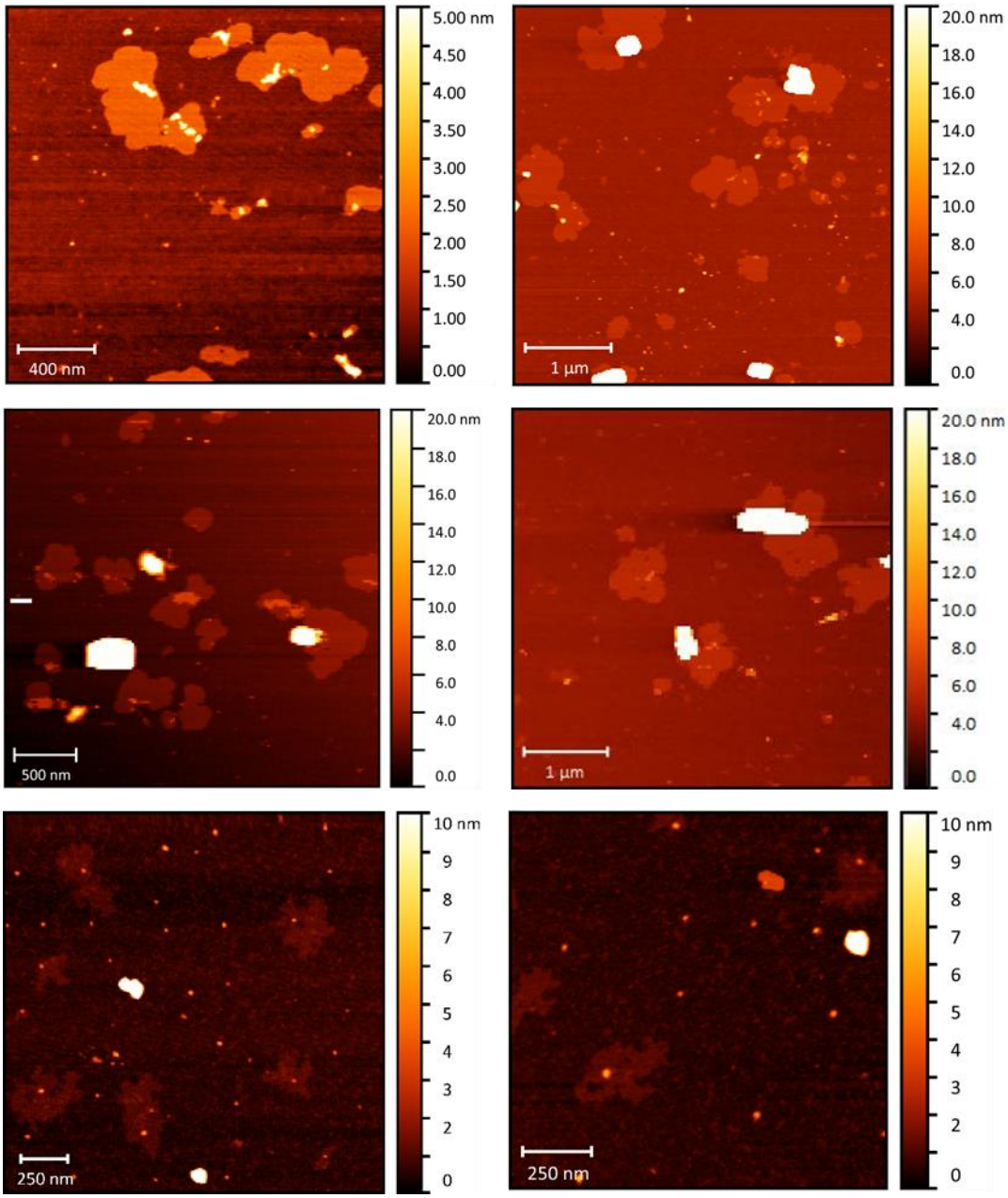

Figure S21. Atomic force microscopy images of exfoliated nanosheets of Cu(ABDC-PS)(DMF).

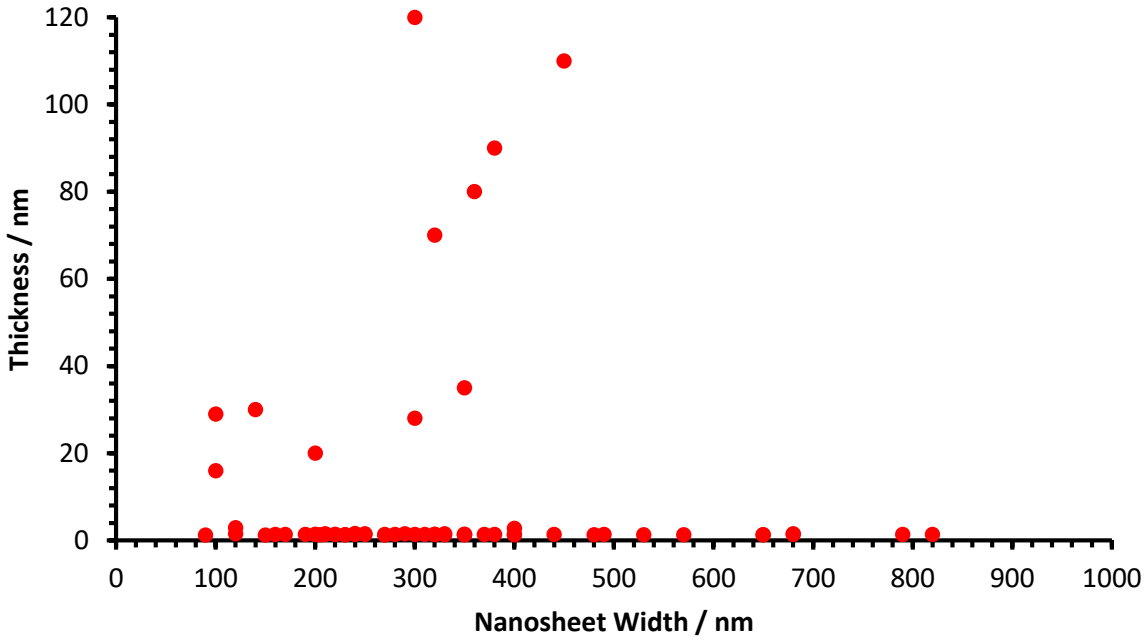

Figure S22. Size distribution scatter graph of Cu(ABDC-PS)(DMF) nanosheets calculated from the above images. The nanosheets consist of predominantly monolayer nanosheets (1.4 nm) alongside occasional poorly exfoliated fragments.

S3.7. Further Analysis of PSF MONs

S3.7.1. FT-IR Spectroscopy

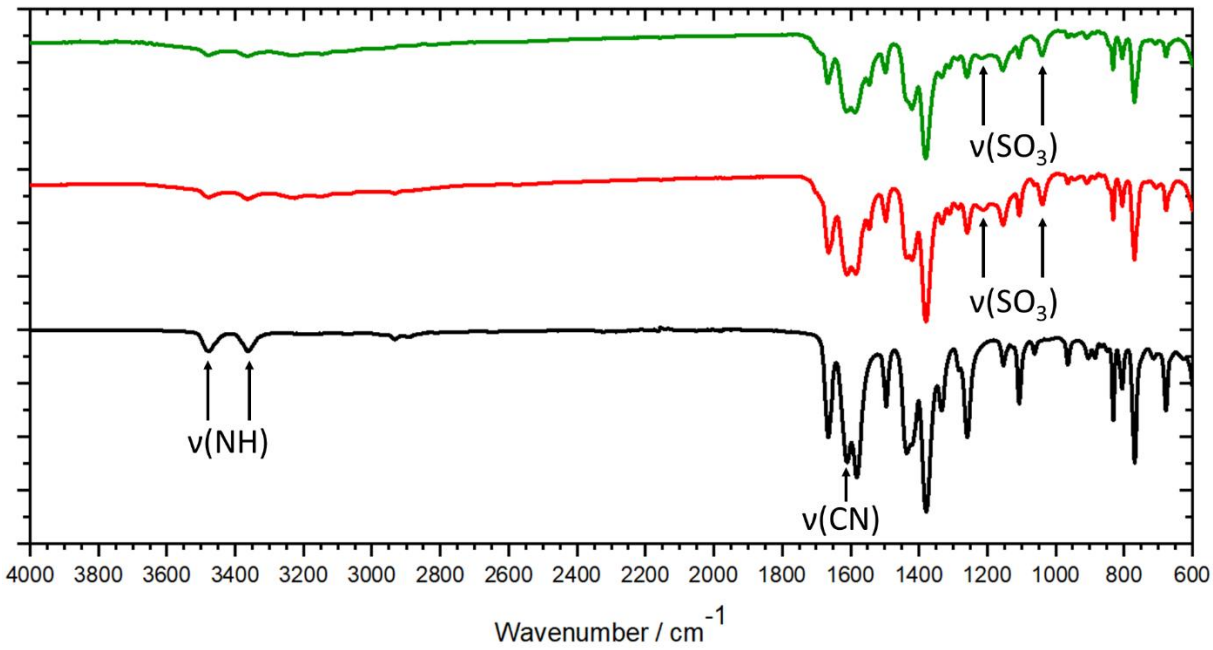

Figure S23. FT-IR spectra of as synthesised Cu(ABDC)(DMF) (black), Cu(ABDC-PS)(DMF) MOF (red) and Cu(ABDC-PS)(DMF) MONs (green), indicating the presence of sulfonic acid stretches in the latter two systems, as according to previous reports.[2–4]

S3.7.2. ^{1}H NMR Spectroscopy

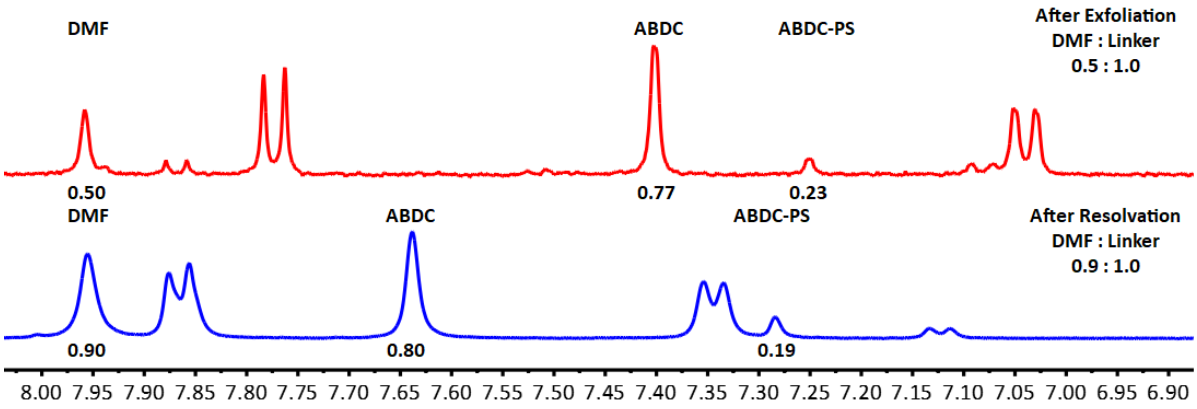

Figure S24. ^{1}H NMR spectrum of digested Cu(ABDC-PS)(DMF) nanosheets (red), indicating approximately 23% functionalisation. The ratio of DMF to MONs is lower than expected (50%) indicating partial desolvation of the MONs during exfoliation. The ^{1}H NMR spectrum of the nanosheets after resolvation with DMF (blue) shows almost full resolvation (90 %). Note that chemical shifts are altered due to the differing amounts of DCl present.

S4. Tandem Catalysis Studies

S4.1. Experimental Details

All catalytic experiments were performed using the same following conditions. Benzaldehyde dimethyl acetal (0.15 mmol), malononitrile (0.40 mmol) and water (0.20 mmol) were each dissolved in d_3-acetonitrile (0.6 mL), treated with catalyst and heated to 60 ^{o}C for 24 hours in sealed reaction vials.

S4.2. Catalysis Yields

Table S3. Yields of each reactant/product for different catalysts using the reaction conditions in S4.1.

Catalyst	Type	[Cat.] / mol%	Yields		
			1	2	3
-	-	0	78	21	1
Cu(ABDC)	MOF	0.2	70	28	1
Cu(ABDC)	MONs	0.1	56	42	2
Cu(ABDC-PS)	MOF	0.2	62	35	3
Cu(ABDC-PS)	MONs	0.1	0	18	82
Cu(ABDC-PS) (and recycled)	MONs	1.5	0 (0)	14 (21)	86 (79)
Cu(ABDC-PS) post-filtration	MONs	0.1	65	32	3

S4.3. 1H NMR Spectra

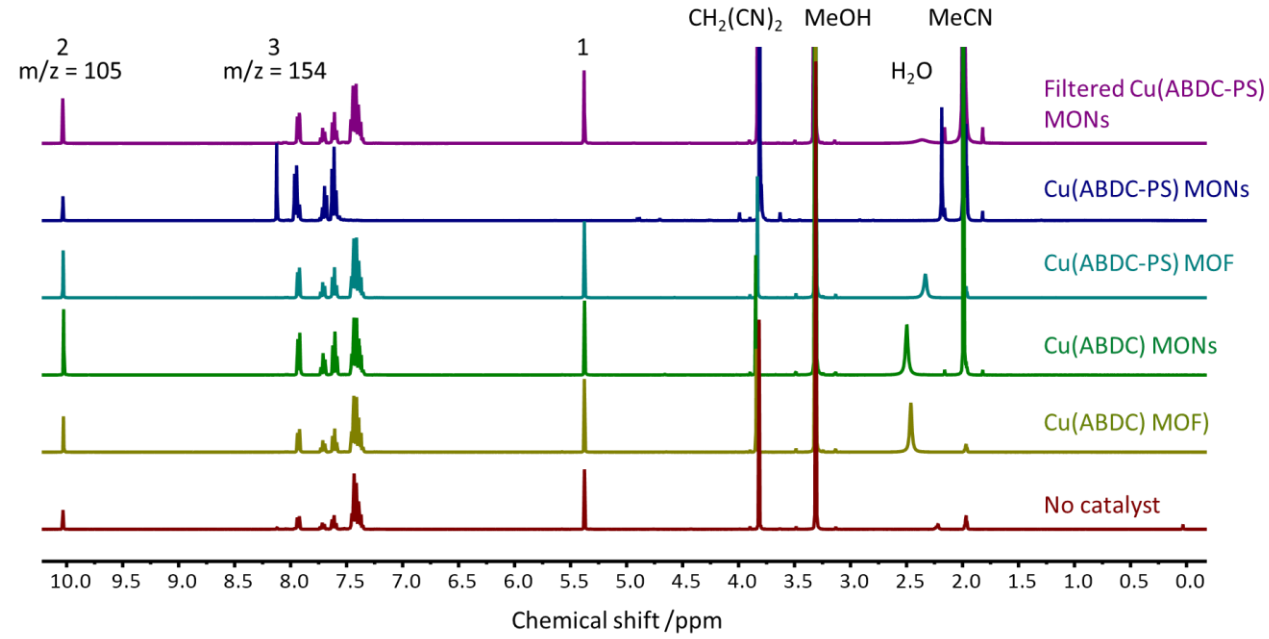

Figure S25. Stacked NMR spectra for each catalytic reaction and control, with characteristic peaks for benzaldehyde dimethyl acetal (1), benzaldehyde (2) and benzylidene malononitrile (3) indicated.

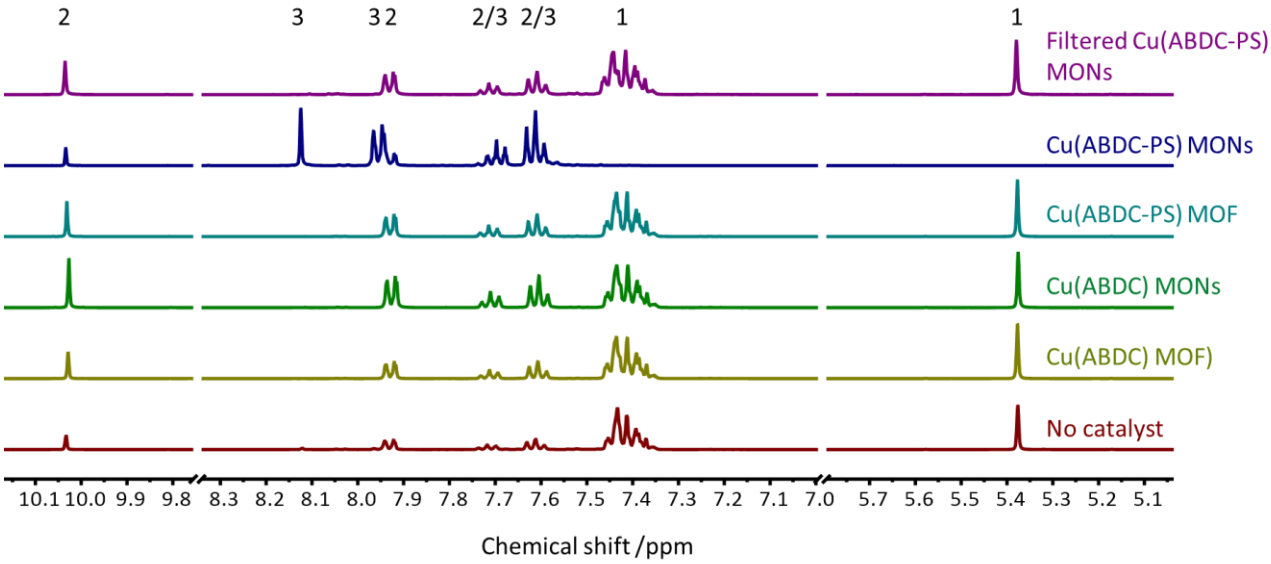

Figure S26. Stacked NMR spectra for each catalytic reaction and control, zoomed in on the region with characteristic peaks for benzaldehyde dimethyl acetal (1), benzaldehyde (2) and benzylidene malononitrile (3).

A suspension of Cu(ABDC-PS)(DMF) nanosheets was filtered through a 0.2 µm Pall® Acrodisc PSF GxF GHP membrane syringe filter three times, leaving a clear solution which exhibited no Tyndall scattering. Without prior dilution, the solution was subject to UV-Vis spectroscopy to determine the concentration of any remaining material (figure S4.4.1). This indicated an approximate concentration of 0.01 $mgmL^{-1}$. There was also an observed redshift in both peaks, perhaps suggesting that the remaining material is actually dissolved material. This sample was

then added to the reaction mixture as for the other catalyst samples to form the Cu(ABDC)(DMF) post-filtration reference.

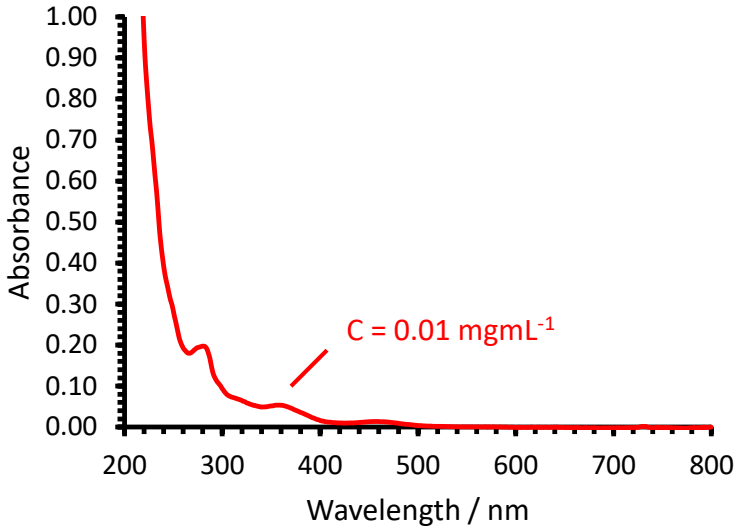

Figure S27. UV-Vis spectrum of the solution obtained from filtration of the Cu(ABDC-PS) nanosheet suspension through a 0.2 µm Pall® Acrodisc PSF GxF GHP membrane syringe filter three times.

S4.4. Recycling Experiments

A catalytic experiment was performed using Cu(ABDC-PS) MONs (1.5 mol%) and otherwise identical conditions to the previous experiments. After 24 hours, the suspension was centrifuged at 4500 rpm to separate the nanosheets, which were washed with acetonitrile and then used again in another catalytic test. The first and second experiments gave 86 and 79 % yields for benzylidene malononitrile respectively, indicating negligible loss of performance upon recycling of the catalyst. NMR spectra are shown in figure S27.

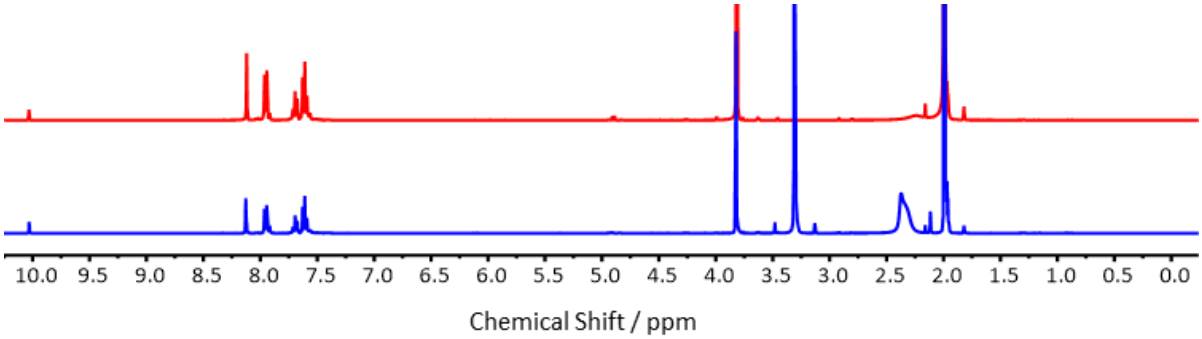

Figure S28. Stacked NMR spectra for mixtures obtained from Cu(ABDC-PS) MONs (1.5 mol%, red), and the same recycled MONs (obtained from centrifugation, blue), under the same conditions, giving 86 and 79 % yields respectively.

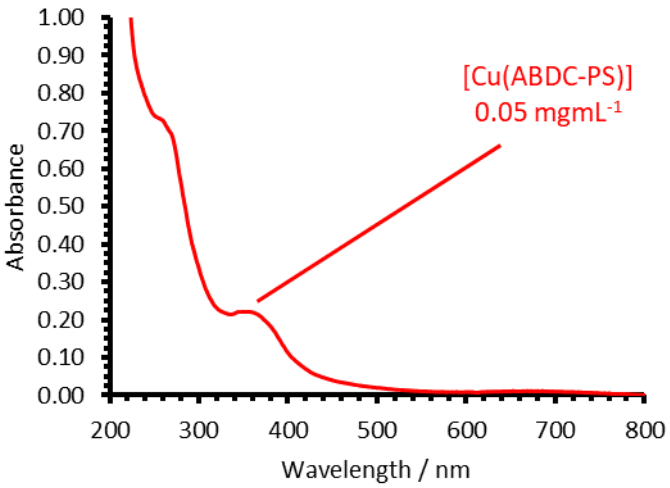

Figure S29. UV-Vis spectrum of material remaining in suspension following centrifugation at 4500 rpm for 3 hours of 1.25 $mgmL^{-1}$ (1.5 mol%) suspension of Cu(ABDC-PS) MONs. The results indicate the majority fo MONs can be recovered by this method with a significantly reduced concentration of 0.05 mg mL^{-1} (no dilution was required).

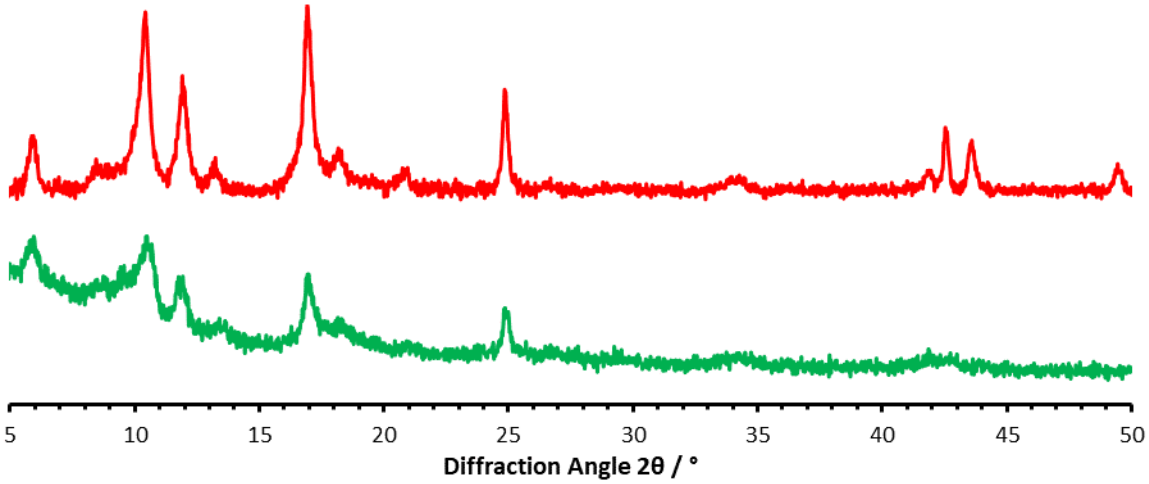

Figure S30. XRPD pattern of Cu(ABDC-PS) MOF (red) and MONs post-catalysis (green), indicating that the structure has been maintained.

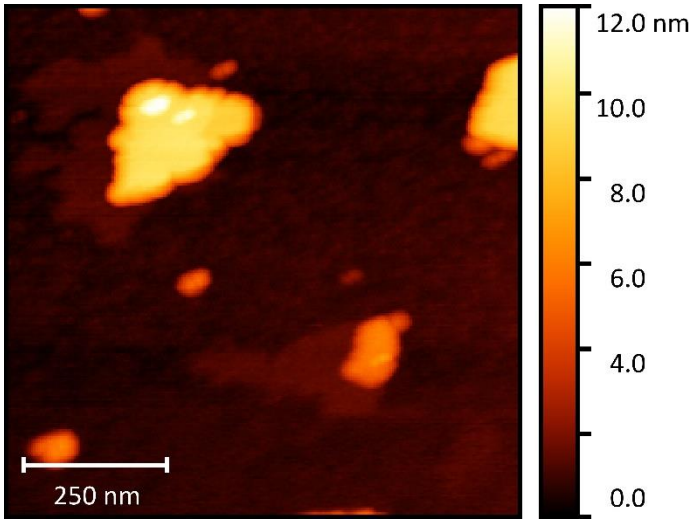

Figure S31. AFM image of Cu(ABDC-PS) MONs post-catalysis.

S5. References

1 M. E. Braun, C. D. Steffek, J. Kim, P. G. Rasmussen and O. M. Yaghi, *Chem. Commun.*, 2001, **2**, 2532–2533.

2 R. S. Andriamitantsoa, J. Wang, W. Dong, H. Gao and G. Wang, *RSC Adv.*, 2016, **6**, 35135–35143.

3 M. Köppen, O. Beyer, S. Wuttke, U. Lüning and N. Stock, *Dalt. Trans.*, 2017, **46**, 8658–8663.

4 H. Liu, F. G. Xi, W. Sun, N. N. Yang and E. Q. Gao, *Inorg. Chem.*, 2016, **55**, 5753–5755.

5 M. Eddaoudi, J. Kim, N. Rosi, D. Vodak, J. Wachter, M. O'Keeffe and O. M. Yaghi, *Science (80)*, 2002, **295**, 469–472.

6 D. J. Ashworth, A. Cooper, M. Trueman, R. W. M. Al-Saedi, S. D. Liam, A. J. Meijer and J. A. Foster, *Chem. - A Eur. J.*, **24**, 68, 17986-17996

7 J. A. Foster, *Chem. Commun.*, 2016, **52**, 10474–10477.

8 J. A. Foster, S. Henke, A. Schneemann, R. A. Fischer and A. K. Cheetham, *Chem. Commun.*, 2016, **52**, 10474–10477.